Applications of Electromagnetic Phenomena in Electrical and Mechanical Systems
S. Yamada, A. Nafalski and S.C. Mukhopadhyay (eds.)

Application of signal cognition for magnetic sensor

Isamu Senoo[1], Y.Saito[1], S.Hayano[1], and I.Marinova[2]
[1]*Graduate School of Engineering, Hosei University, 3-7-2 Kajino, Koganei, Tokyo, 184-8584,Japan*
[2]*Department of Electrical Apparatus, Technical University of Sofia, Sofia 1756,Bulgaria,*
seno@ysaitoh.k.hosei.ac.jp

ABSTRACT: In this paper, we apply the image cognition technology of the human voice to the cognition of the magnetic sensor signals. At first, the time domain signals are converted into the three-dimensional images, which construct the database system. Secondly, when we measure a time domain signal, this signal is also converted into a three-dimensional image. This three-dimensional image becomes an input vector of a least square means. Least squares solution gives a composite signal as a linearly combined database signals. Extracting the most dominant term from the least squares solution reveals the cognized signal. Thus, we have succeeded in the time domain signal cognition by means of the image cognitive technology.

1 INTRODUCTION

Magnetic Sensor can be classified into two major categories depending on the applications. One is the nondestructive use for the metallic materials. The other is the magnetization characteristic measurements use. The former is based on the principle that detects the disturbance of the magnetic distributions caused by the magnetization vectors in the magnetic materials or by the eddy currents induced by the alternating magnetic fields. The latter is also based on the similar principle, but it have to detect the precise magnetic quantities, e.g. magnetization vectors or flux. Both sensors require the handling technique of electrical signals representing the physical properties of the target material.

Principal purpose of this paper is to introduce a new signal handling methodology of the magnetic sensors based on an image processing technique [1]. By means of our new signal handling technique, we try to classify the cans depending on their physical property as well as size.

In order to convert the magnetic sensor signals into the three-dimensional images, we propose a three-dimensional Lissajous, which counts the overlapped points while conventional Lissajous does not take into account the overlapped points in a two-dimensional plane. The magnetic sensor signal contains various information concerning with a target physical properties, i.e. physical dimensions, magnetic or not magnetic materials. Our three-dimensional Lissajous methodology makes it possible to cognize the distinct physical property in each of the targets.

As a result, it is revealed that least squares mean along with three-dimensional Lissajous not only improves the sensibility of magnetic sensor but also cognizes the physical dimensions as well as properties.

2 MAGNETIC SENSOR

2.1 Operating principle

Table 1. Various constants of a tested sensor

Coil	Number of turns	Coil diameter	Coil length	Material of Coils
Exciting coil	211	90mm	100mm	Enameled wire with 0.8mm diameter
Sensing coils	145	90mm	50mm	Enameled wire with 0.6mm diameter

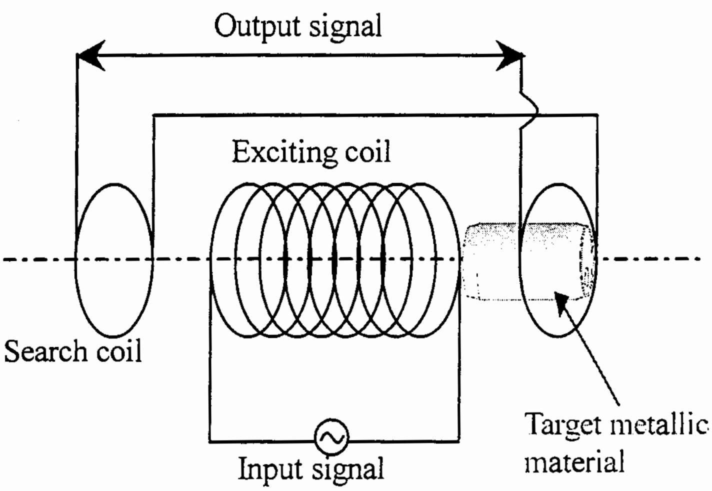

Fig. 1. Schematic diagram of a sensor

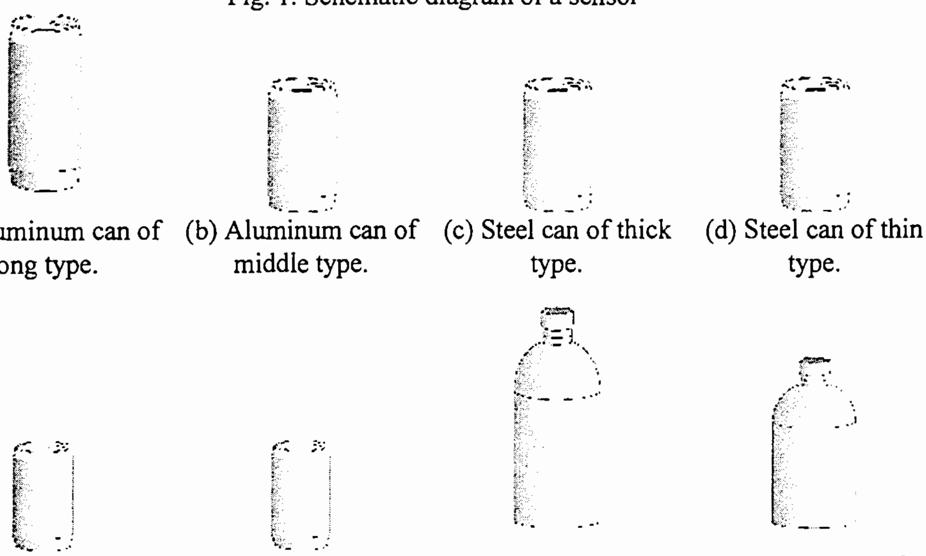

(a) Aluminum can of long type. (b) Aluminum can of middle type. (c) Steel can of thick type. (d) Steel can of thin type.

(e) Steel can of small type. (f) Steel can of small type. (g) Aluminum stein can of long type. (h) Aluminum stein can of middle type.

Fig. 2. Target metallic materials

Figure 1 shows a schematic diagram of the magnetic sensor. This sensor is composed of an exciting coil, two sensing coils connected in differentially, and targets. When alternating current is flowing into the exciting coil and a target metallic material locates at a center of exciting coil, no induced voltage is observed at the sensing coils because sensing coils are differentially connected and their linkage magnetic fluxes are the same. However, when the target metallic material locates at any position along with an exciting coil axes excepting the center of exciting coil, a difference of the magnetic flux linkages between the left- and right-sided sensing coils yields a sensing signal. This is a basic operating principle of this magnetic sensor. Table 1 lists the specification of our tested sensor. Figure 2 shows 8 kinds of can used as targets.

2.2 Input and output signals

Figure 3 shows an input sinusoidal voltage having 100kHz frequency, 4V peak amplitude and typical output signal when having no target. Figure 4 shows the sensor output signals when one of the target cans in Fig.2 locates at the inside of the right side sensing coil. Comparison of the input with the output signals reveals that any of the output signals contain a relatively higher frequency noise.

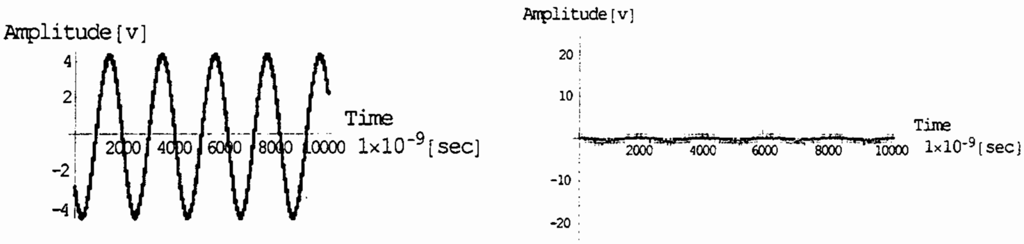

(a) Input signal. (b) Output signal.

Fig. 3. Input and output signals without any target

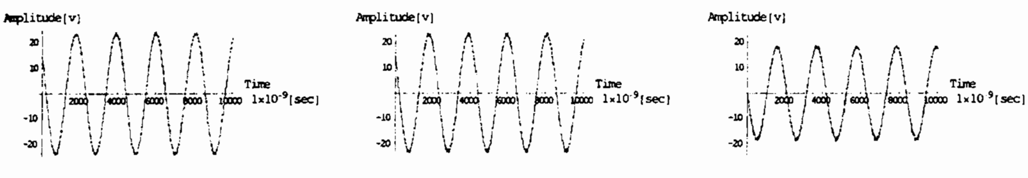

(a) Aluminum can of long type. (b) Aluminum can of middle type. (c) Steel can of thick type.

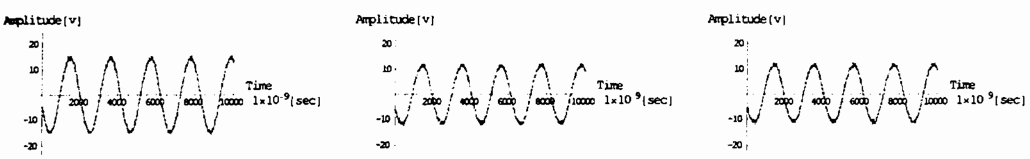

(d) Steel can of thin type. (e) Steel can of small type. (f) Steel can of small type.

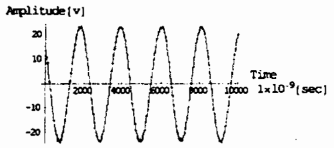

(g) Aluminum stein can of long type.

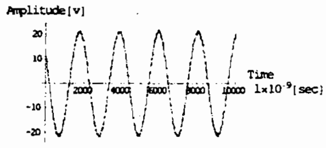

(h) Aluminum stein can of middle type.

Fig. 4. Output signals when one of the target cans in Fig.2 locates at the inside of the right side sensing coil

3 SENSOR SIGNAL COGNITION

3.1 Three-Dimensional Lissajous diagram

To remove the time phase difference of sensor signals, one of the best ways is to draw a Lissajous diagram. Further, if only one-dimensional time series signal is considered, then all of the signal information, e.g. amplitude, frequency, and phase information, is included in one-dimensional time series signal. Thereby, Lissajous diagram is one of the best diagrammatic ways, which is capable of representing the frequency ratio, amplitude and phase difference information on two signals.

By taking the one time dependent signal to the x-axis and the other time dependent signal to the y-axis we can draw the Lissajous diagram. For example, when the same signals are taken to the x- and y-axis, the Lissajous diagram becomes a simple straight line as shown in Fig.5 (a). In Lissajous diagram, amplitude, phase and frequency information are reflected on its magnitude, tilt angle and shape, respectively. Figure 5 shows typical examples of conventional Lissajous diagram. It is found out from observing the Lissajous diagrams in Fig. 5, two signals are essential to draw the Lissajous diagram. The phase difference of these signals yields different shapes of diagrams, for examples, elliptic Lissajous diagram shown in Fig.5 (b) when phase difference is 45 degrees, circular Lissajous diagram shown in Fig. 5(c) when phase difference is 90 degrees.

From a viewpoint of image, it is obvious that the circular Lissajous diagram shown in Fig. 5(c) has rich information as an image, because the circular Lissajous diagram occupies large area on an image. If only one signal is available like a voice signal, then integration or differential operation makes it possible to draw a circular Lissajous diagram [2]. However, our tested magnetic sensor, shown in Fig.1, has two signals, i.e., input and output signals as shown in Fig.3, so that it is possible to draw a Lissajous diagram.

One of the weak points of conventional Lissajous diagram is that it looses the information concerning with overlapped points. Thus, the conventional Lissajous diagram is regarded one of the binary images that are consisted data of just one and zero. However, when we take into account the overlapped points information by means of the simple sum operation, i.e., histogram, it is possible to draw a three-dimensional Lissajous diagram, which can be regarded as one of the three-dimensional images having rich information. Since sum operation corresponds to integral in discrete mathematics, then this operation not only increases the amount of information but also removes effect of noise. When we apply to the signal without periodicity, it is possible to draw a light and shadow drawing, which is called three-dimensional image in this paper. We have previously reported that this three-dimensional image method is an effective tool to cognize human voice signals even though sound echo environments are changed.

Figure 6 shows the effects of phase difference in three-dimensional Lissajous diagram. Also, Figure 7 shows the three-dimensional Lissajous diagrams between the input signal in Fig. 3(a) and each of the output signals in Fig.4.

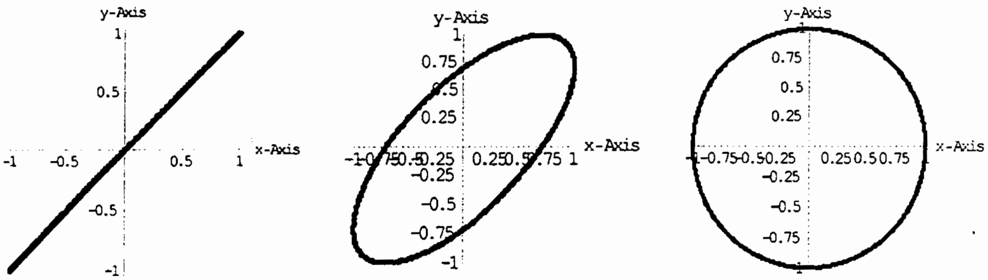

(a) In phase. (b) 45 degrees difference. (c) 90 degrees difference.

Fig. 5. Typical examples of conventional Lissajous diagram

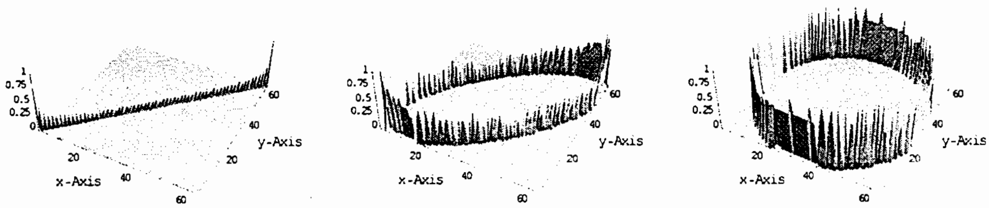

(a) Same phase. (b) 45 degrees difference. (c) 90 degrees difference.

Fig. 6. Effects of phase differences in 3D Lissajous diagram.

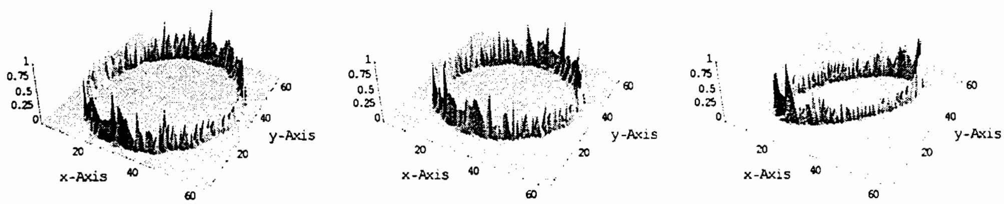

(a) Aluminum can of long type. (b) Aluminum can of middle type. (c) Steel can of thick type.

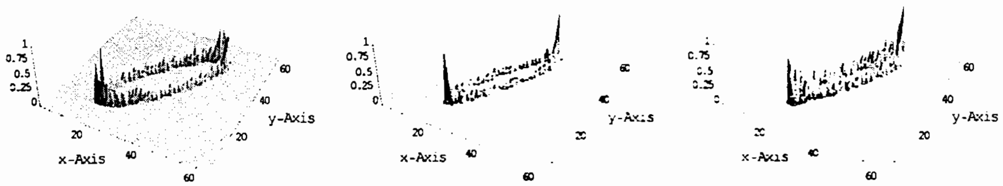

(d) Steel can of thin type. (e) Steel can of small type. (f) Steel can of small type.

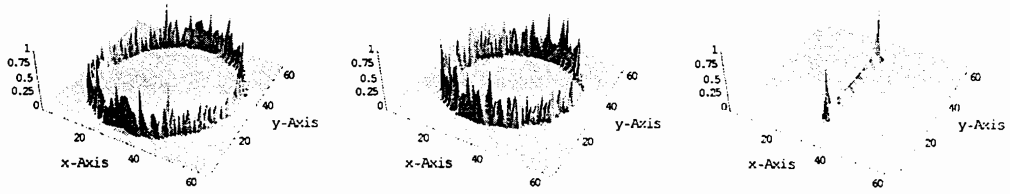

(g) Aluminum stein can of long type. (h) Aluminum stein can of middle type. (i) Without any cans.

Fig. 7. Three-dimensional Lissajous diagrams between the input signal in Fig. 3(a) and each of the output signals in Fig.4

3.2 Least Squares Solution

When we regard the three-dimensional Lissajous diagrams as image data having 64 by 64 resolution, it is possible to apply the image cognitive technology [2]. To apply our image cognitive technology, each of the image data is rearranged into a column-wise form, which constitutes an image vector $c_i, i = 1,2,.,n,$ with order 4096, where n is a number of images. Thus, we have a system matrix C as

$$C = [\mathbf{c}_1, \mathbf{c}_2,., \mathbf{c}_n]. \quad (1)$$

Similarly, denoting an input image vector Y yields a following system of equations:

$$\mathbf{Y} = C\mathbf{X} \quad (2)$$

where the solution vector X is composed of n elements.

If a condition

$$n < 4096 \quad (3)$$

is held, then a least squares solution

$$\mathbf{X} = \left(C^T C\right)^{-1} C^T \mathbf{Y} \quad (4)$$

minimizing a least squares error

$$\varepsilon = \sqrt{\mathbf{Y} - C\mathbf{X}} \quad (5)$$

could be obtained[3].

The magnitude of elements in the solution vector $\mathbf{X}$ suggests a cognized image vector. Namely, the biggest element in the solution vector $\mathbf{X}$ reveals the cognized image.

3.3 Classification of Target Metallic Cans

We have carried out the measurements of sensor output signals changing 8 kinds of can and without any cans. This yielded 9 three-dimensional Lissajous images, which constructed a rectangular system matrix C with 4096 rows and 9 columns. When we construct the input vector $\mathbf{Y}$ from the column vector $c_i, i = 1,2,.,9$, it is possible to classify the exact kind of can for any input vector $\mathbf{Y}$ by Eq. (4).

However, the noise included in the sensor output signals measured practically does not have any regularity, which depends on the electromagnetic environments. This means that the same sensor output signal is never obtained even if the same kind of can.

To check up the validity of our methodology, we have carried out 5 times measurements of same kind of cans changing the electromagnetic environments. Using these sensor output signals, we have carried out the classification of cans. Fig. 8 shows the elements in the solution vector $\mathbf{X}$.

Observation of the results in Fig. 8 reveals that fairly good solutions are obtained by the least squares mean. Taking the biggest element in each of the solution vector $\mathbf{X}$ makes it possible to classify the distinct target can. Further observation of the results in Fig.8, it is found that the maximum element in the solution vectors of Figs. 8(e) and 8(f) takes the 5^{th} element. This is because the quality of the material and the form of the 5^{th} and 6^{th} cans are the same as shown in Figs. 2,4 and 7.

Thus, we have succeeded in cognizing each of the target cans by our new method.

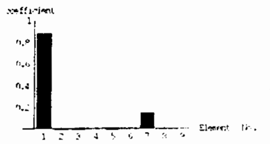

(a) Aluminum can of long type.

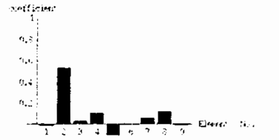

(b) Aluminum can of middle type.

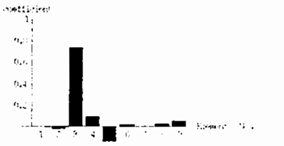

(c) Steel can of thick type.

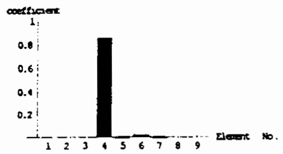

(d) Steel can of thin type.

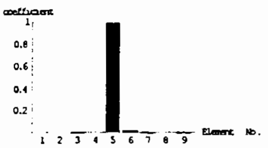

(e) Steel can of small type.

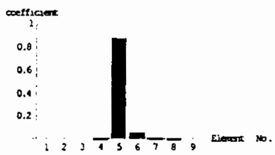

(f) Steel can of small type.

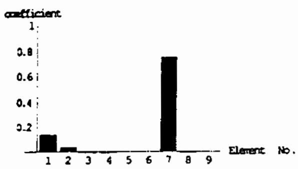

(g) Aluminum stein can of long type.

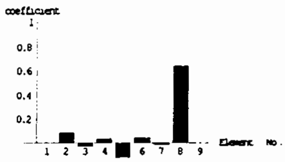

(h) Aluminum stein can of middle type.

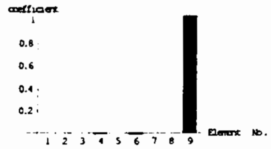

(i) Without any cans.

Fig. 8. Elements of the solution vector $\mathbf{X}$

4 CONCLUTION

We have proposed a new signal processing methodology along with the three-dimensional Lissajous diagram. In this paper, our proposed method has been applied to the magnetic sensor signals to classify the different kind of metallic cans. As a result, a fairly good result has been obtained as an initial test.

Until now, it is essentially required a skillful engineer to classify the metallic cans. An automatic machine employing our new signal processing methodology may replace this human intelligence oriented technology.

5 REFERENCES

[1] I.Senoo, S.Hayano, Y.Saito, "Magnetic sensor signal analysis based on an image processing method", *Paper on technical meeting of Magnetics Society of IEEJ*, MAG-00-115, July 2000.

[2] I.Senoo, S.Hayano, Y.Saito, "Voice cognition by wavelets image processing", Paper No. P1-008, *Japanese Visualization Technology Symposium*, July 17th 2000.

[3] H.Takahashi, S.Hayano, Y.Saito, "Visualization of the Currents on The Printed Circuit Board", *IEEE Visualization 1999, Late Breaking Hot Topics*, pp.37-40, Oct. 1999.